JBC RESEARCH ARTICLE

The structural dynamics of full-length divisome transmembrane proteins FtsQ, FtsB, and FtsL in FtsQBL complex formation

Received for publication, April 2, 2022, and in revised form, June 28, 2022 Published, Papers in Press, July 4, 2022,
https://doi.org/10.1016/j.jbc.2022.102235

Wai-Po Kong, Furong Gong, Pui-Kin So, Yu Wai Chen, Pak-Ho Chan, Yun-Chung Leung, and Kwok-Yin Wong*

State Key Laboratory of Chemical Biology and Drug Discovery, Department of Applied Biology and Chemical Technology, The Hong Kong Polytechnic University, Kowloon, Hong Kong, China

Edited by Wolfgang Peti

FtsQBL is a transmembrane protein complex in the divisome of *Escherichia coli* that plays a critical role in regulating cell division. Although extensive efforts have been made to investigate the interactions between the three involved proteins, FtsQ, FtsB, and FtsL, the detailed interaction mechanism is still poorly understood. In this study, we used hydrogen-deuterium exchange mass spectrometry to investigate these full-length proteins and their complexes. We also dissected the structural dynamic changes and the related binding interfaces within the complexes. Our data revealed that FtsB and FtsL interact at both the periplasmic and transmembrane regions to form a stable complex. Furthermore, the periplasmic region of FtsB underwent significant conformational changes. With the help of computational modeling, our results suggest that FtsBL complexation may bring the respective constriction control domains (CCDs) in close proximity. We show that when FtsBL adopts a coiled-coil structure, the CCDs are fixed at a vertical position relative to the membrane surface; thus, this conformational change may be essential for FtsBL's interaction with other divisome proteins. In the FtsQBL complex, intriguingly, we show only FtsB interacts with FtsQ at its C-terminal region, which stiffens a large area of the β-domain of FtsQ. Consistent with this, we found the connection between the α- and β-domains in FtsQ is also strengthened in the complex. Overall, the present study provides important experimental evidence detailing the local interactions between the full-length FtsB, FtsL, and FtsQ protein, as well as valuable insights into the roles of FtsQBL complexation in regulating divisome activity.

Bacterial cell fission proceeds through a complex machinery called divisome (1). In *Escherichia coli*, the divisome is composed of over 30 proteins, about ten of which are essential (2). These protein components assemble at the midcell following a hierarchical order: FtsZ > FtsA > ZipA/ZapA > FtsK > FtsQ > FtsB/FtsL > FtsW > FtsI (PBP3) > FtsN (3–5). Upon these proteins working in a well-coordinated manner, the mother bacterium can undergo cytokinesis, constriction, and septation and divide into two daughter cells (6).

FtsQ, FtsB, and FtsL are inner-membrane proteins that interact at the midcell and are critical for cell divisions (7, 8). In the divisome, the FtsQBL complex, which was proposed to form with stoichiometry of 1:1:1 (9, 10) or 2:2:2 (10, 11), serves as a scaffold essential for recruiting downstream proteins (FtsW, FtsI, and FtsN) and plays a critical role in regulating septal-peptidoglycan (sPG) biosynthesis (12). Mutagenesis studies have identified the constriction control domains (CCDs) in FtsB (residues 55–59) and FtsL (residues 88–94) (6). Some of those mutants can override the depletion of essential FtsN activation and survive in the absence of the FtsN-essential domain (^{E}FtsN) (13). Considering that ^{E}FtsN is likely to be the stimulator facilitating the sPG biosynthesis, it has been hypothesized that FtsQBL may have two conformations, the 'off' and 'on' states, to regulate the downstream proteins (6, 14, 15). FtsQBL in the default 'off' state inhibits the PBP1b-FtsW-PBP3 activity to prevent premature cell separation (13). Interactions with FtsA and FtsN switch the FtsQBL conformation into the 'on' state and promote sPG biosynthesis (6, 13). The FtsBL subcomplex can directly regulate the PBP1b activity that can be enhanced by the addition of FtsQ (12).

Although significant research efforts have been devoted to investigating the interactions among FtsQ, FtsB, and FtsL, the detailed mechanism remains obscure. FtsQ, FtsB, and FtsL are type II bitopic membrane proteins with a periplasmic domain and a relatively short cytoplasmic domain. FtsQ is the largest one consisting of a cytoplasmic N-terminal domain (residues 1–24), a transmembrane (TM) domain (residues 25–49), and a large periplasmic domain (residues 50–276) (16–18). The periplasmic domain consists of the α- and β-domains (19). The α-domain resembles a polypeptide transport-associated (POTRA) subdomain (20) and is essential for localizing FtsQ to the midcell through the interactions with another essential upstream protein, FtsK (21). The β-domain, on the other hand, is responsible for recruiting downstream proteins. This domain is vital for the FtsQBL complex formation (10, 22) and suppressing the PBP3 TPase activity (12). FtsB and FtsL, in contrast, are small proteins of similar sizes and domain organizations. There is only limited information on the structures and functions of these two proteins. Some structures of FtsB have been

* For correspondence: Kwok-Yin Wong, kwok-yin.wong@polyu.edu.hk.

© 2022 THE AUTHORS. Published by Elsevier Inc on behalf of American Society for Biochemistry and Molecular Biology. This is an open access article under the CC BY-NC-ND license (http://creativecommons.org/licenses/by-nc-nd/4.0/).

reported (10, 23, 24), whereas no structure of FtsL is currently available. The COILS program has suggested that both the FtsB and FtsL periplasmic regions contain characteristics of coils (25). A recent coevolutionary study has also indicated that FtsL is possibly a continuous helix across the TM and periplasmic domain (11). FtsB and FtsL are interdependent for stabilization and form a stable complex before binding to FtsQ (8, 26). The FtsBL complex formation has been suggested to be mediated by the TM region (27) and the predicted leucine-zipper motifs in both proteins (11, 28). On the other hand, the periplasmic domains of FtsB and FtsQ can form a complex in the absence of FtsL (9) that also enhances the FtsB-FtsL affinity (24). Unfortunately, most studies were either indirect or based on truncated proteins. This prompted us to investigate the interactions and dynamics with the full-length complex, which is essential for understanding the modes of FtsQBL action.

Herein, we report our study on the structural dynamics of the full-length FtsQBL complexation through hydrogen-deuterium exchange (HDX) mass spectrometry (MS). The kinetics of HDX is dependent on the appearance of binding, secondary structure, structural rigidity, and solvent accessibility of the protein (29). This technique allows the detection of subtle changes in the protein structure and dynamics under different conditions (29–33). To investigate the protein–protein interactions among FtsQ, FtsB, and FtsL, the HDX kinetics were monitored separately in the free and complexed state. The changes in protein conformational dynamics and/or solvent accessibility due to direct binding were determined by comparing the local deuterium uptake with and without complexation. The interpretation of the HDX-MS data was aided by complex structure prediction and molecular modeling. This information provides insight into the mechanism of the interactions upon the FtsQBL complexation.

Results

FtsQBL complex formation

To investigate the interactions among FtsQ, FtsB, and FtsL, the HDX behavior of each individual protein was compared with that in the respective FtsQBL complexed state. The labeled proteins were treated by online pepsin digestion, followed by LC-MS analysis. This method resulted in reproducible results with acceptable peptide coverage of FtsQ (61.2%), FtsB (83.2%), and FtsL (76.3%) (Fig. S4). Figure 1, *A*–*C* show the differences in deuterium uptake between the proteins in the free and FtsQBL complexed states. The HDX-MS data were mapped onto a three-dimensional model. The detailed procedures of protein purifications, HDX-MS experiments, recovery of the peptic peptides, and model construction can be found in the Supporting information (Figs. S5–S15).

An overall deuteration decrement was detected in FtsQ upon the complexation with FtsB and FtsL (Fig. 1*A*). Regions of S3 to S5 and S8 to S12 with helix H4 in FtsQ were protected against the deuterium exchange in the complexed state. Compared with that in the free-state protein, at least 0.7 Da of deuteration reduction was observed in fragments 124 to 132, 124 to 139, 126 to 132, and 128 to 139 after complexation. These related residues cover the loop-dominant region (S3–S5) between the α- and β-domains in FtsQ. Other peptides with HDX decrements were found at the C-terminal region: 187 to 193, 194 to 203, 196 to 203, 207 to 216, 209 to 223, 231 to 243, and 247 to 263. Predominant uptake changes up to 3 Da appeared in the FtsQBL-state, indicating that the interaction with FtsB and FtsL protected the FtsQ C terminus S8 to S12 from deuteration. Taken together, the binding with FtsB and FtsL reduced the deuterium uptake of FtsQ at the upper β-domain (residues 187–263) and the lower β-domain (residues 124–139).

For FtsB, an overall decline of HDX was observed upon FtsQBL complexation (Fig. 1*B*). A substantial decrement can be found in a series of peptides corresponding to the TM domain and the nearby periplasmic region when compared between the free and the FtsQBL complex states. Significant uptake reductions (0.5–1.1 Da) appeared in the peptides related to the TM domain (residues 4–21) (23, 34) at the 1 min interval, including fragments −1 to 6, −1 to 19, and 20 to 28. The FtsQBL complexation leads to a more pronounced HDX decrement in the lower periplasmic region. A noticeable deuteration reduction appeared in peptides from residues 29 to 54 (Fig. 1*B*). The differences of deuterium uptake level in the corresponding peptides ranged from 1.6 to 8.9 Da. Moreover, the C terminus was protected from deuteration. Peptic peptides (76–84 and 77–84) incorporated 0.5 and 0.3 Da less in the FtsQBL complex relative to the free state at the time interval of 1 min.

The HDX results revealed that FtsL is also protected from deuterium exchange upon FtsQBL formation (Fig. 1*C*). An uptake decrement appeared in peptides with residues across the TM domain and the lower periplasmic region. Peptide fragments covering residues 33 to 86 showed a considerable HDX reduction in the complexed state. Similar to the protection pattern in FtsB (Fig. 1*B*), the FtsQBL complexation has different impacts on the two regions of FtsL; a noticeable reduction of HDX (∼1 Da) appeared in the TM region (residues 33–57) (27, 35), whereas a more significant change (>2 Da reduction) in the adjacent periplasmic region (residue 62–86) is observed at the 1 min interval.

FtsBL subcomplex formation

To further investigate the details, the HDX profile of the FtsBL subcomplex was analyzed by comparing it with the FtsB and FtsL in the corresponding free state (Fig. 2). The HDX decrements were observed in the TM and lower periplasmic domains of both FtsB and FtsL. Specifically, the reductions in deuterium uptake that occurred in FtsB (residues 1–60) and FtsL (residues 33–86) in the FtsBL subcomplex were similar to those in the FtsQBL complex (by comparison of Fig. 2, *A* and *B* with Fig. 1, *B* and *C*). However, unlike the peptides that were in the FtsQBL complex (Fig. 1*B*), no significant uptake difference was observed at the FtsB C-terminal region in the FtsBL subcomplex. Thus, most of the protections in FtsB and FtsL were probably caused by the FtsBL subcomplex formation through the TM domain and their juxtaposed periplasmic region (Fig. 2*D*).

ASBMB

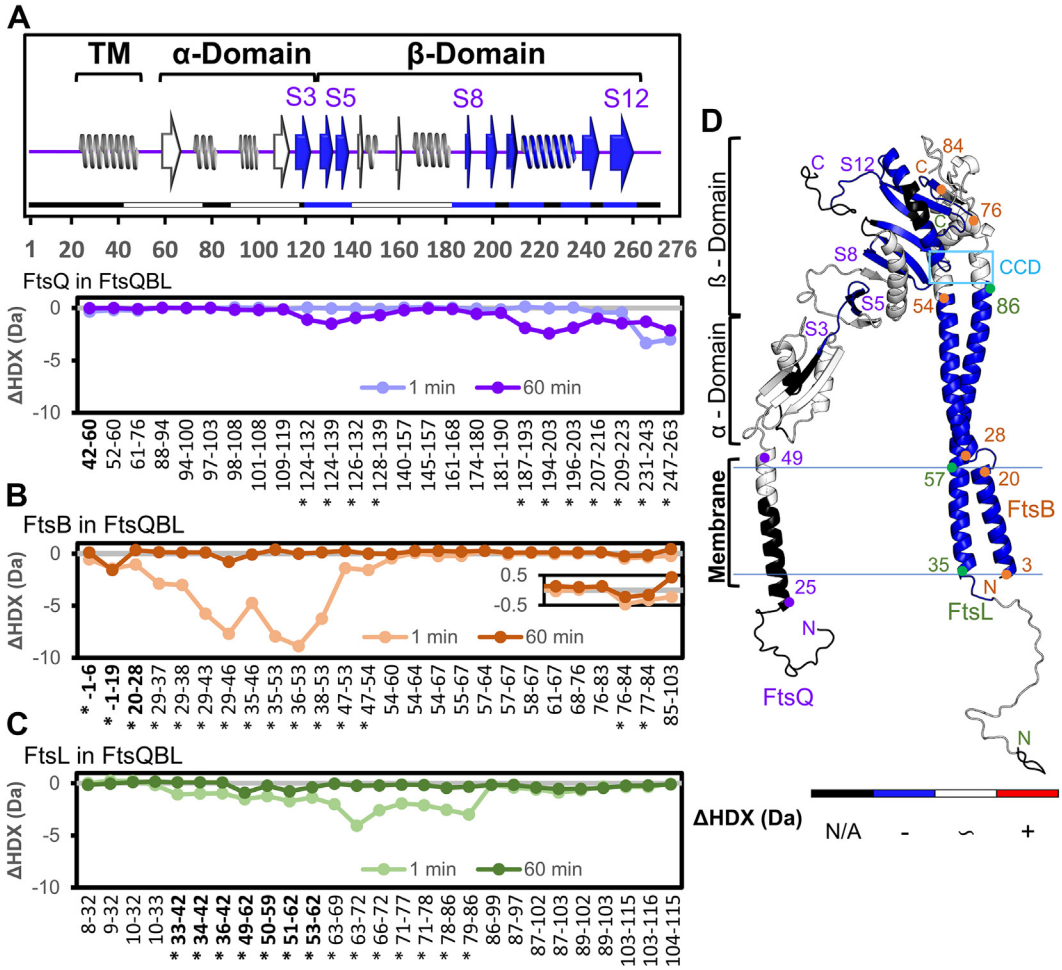

Figure 1. The dynamics of the FtsQBL complex monitored by HDX-MS. The peptide deuterium uptake differences (ΔHDX, FtsQBL-complexed state minus the free states) of (*A*) FtsQ with the secondary structure showed on *top*, (*B*) FtsB, and (*C*) FtsL, at 1 min and 60 min time intervals. The peptides related to the predicted TM regions are in *bold*. Peptides with significant ΔHDX are marked with an *asterisk*. The general coloring scheme for the ΔHDX plots of the three proteins are as follows: FtsQ (*purple*); FtsB (*orange*); FtsL (*green*). *D*, model of the FtsQBL complex with mapped ΔHDX. Peptides showing a HDX decrement, an increment, and no significant difference are in *blue*, *red*, and *white*, respectively; while the missing fragments are in *black*. This information is also included with the same color scheme in the bar of (*A*). HDX, hydrogen-deuterium exchange; MS, mass spectrometry; TM, transmembrane.

Furthermore, the uptake profiles also provided an additional layer of dynamical information in the FtsBL complex formation (Fig. 2). Interestingly, only some peptides within the TM regions showed protection after a prolonged period of HDX (60 min). Upon interactions, all the TM peptides of FtsB and FtsL demonstrate a significant uptake reduction after 1 min of deuteration. Ten of these peptides had HDX protection (>0.45 Da) at the 60 min of labeling. In particular, peptic fragments near the periplasmic region (FtsB −1 to 19; FtsL 49–62, 50–59, 51–62, and 53–62) remain protected at the 60 min time interval. Meanwhile, the remaining four peptides in FtsB (−1 to 6) and FtsL (33–42, 34–42, and 36–42) showed no difference after extended labeling. The distinct changes of deuterium uptake kinetics may reflect different dynamic changes in the corresponding region (36). It can be inferred that the residues near the periplasmic domain are better protected from HDX than those near the cytoplasmic surface that bind tighter or are stiffer in the FtsBL subcomplex.

Consistent with the results of the TM peptides, HDX decrements were found at the FtsB and FtsL TM-proximal periplasmic regions: FtsB (residues 22–54) and FtsL (residues 58–86). The deuterium incorporation of the crossregion fragments (FtsB [20–28] and FtsL [53–62]) was moderately reduced by about 1 Da in the first minute. Considerable uptake decrements were found in the juxtaposed periplasmic peptides from residues 29 to 54 (FtsB) and 63 to 78 (FtsL) with at least 1.2 and 1.9 Da, respectively. A maximum of 8.5 and 3.7 Da decrement can be observed in the fragment from the lower periplasmic region of FtsB and FtsL, respectively. Together with the observations from the TM domains, our results reveal that FtsB and FtsL mutually protect large areas from deuteration. The formation of the FtsBL subcomplex is presumably accomplished by a continuous interface across the TM domain and the adjacent periplasmic regions (up to Phe54 of FtsB and Leu86 of FtsL). This binding mode of FtsB-FtsL is supported by the previous speculation that both the TM residues and their nearby coiled-coil domains contribute to the FtsBL interaction (8, 9, 11, 17, 25, 27, 28, 35, 37, 38). However, we did not observe the involvement of the 'last leucine zipper unit' in FtsB (residues 55–72), which was hypothesized to interact with FtsL previously (8, 28, 37).

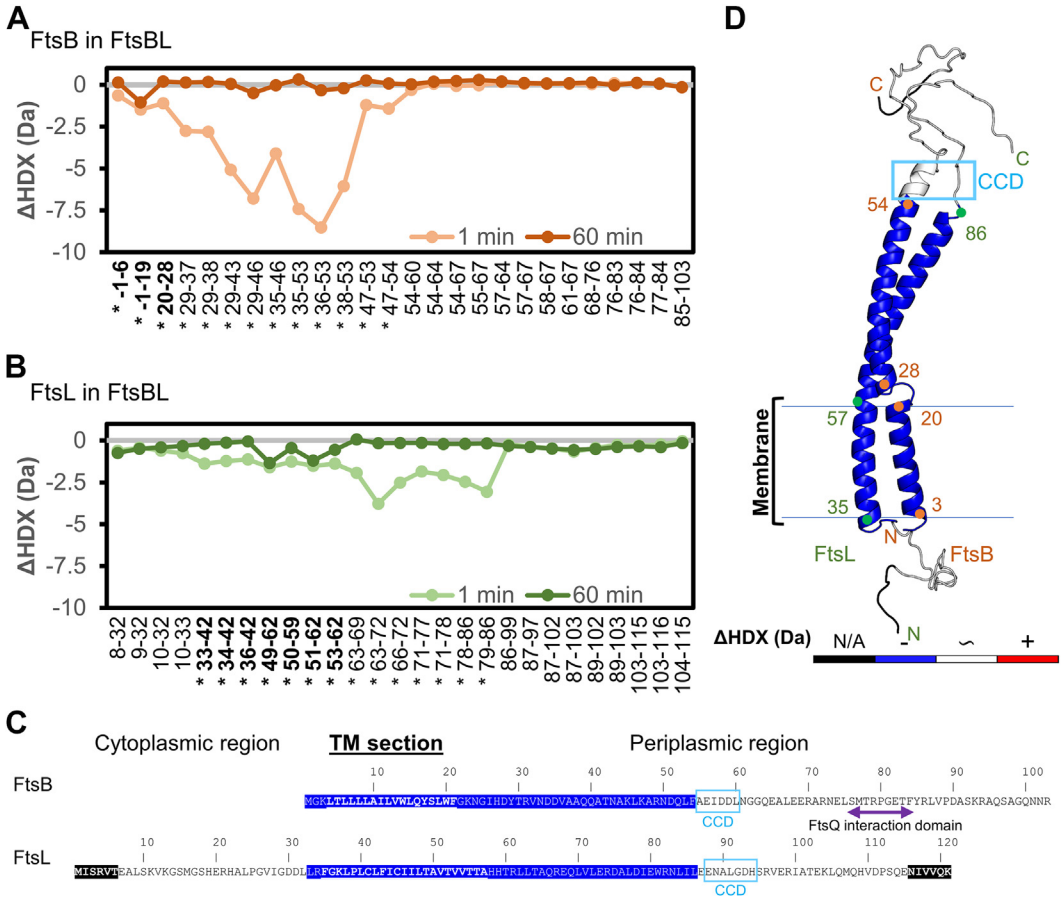

Figure 2. The dynamics of the FtsBL complex monitored by HDX-MS. The peptide deuterium uptake difference (ΔHDX, FtsBL-complexed state minus the free states) of (*A*) FtsB and (*B*) FtsL. The peptides related to the predicted TM regions are in *bold*. Peptides with significate ΔHDX are marked with an *asterisk*. The general coloring scheme for the ΔHDX plots of the two proteins are as follows: FtsB (*orange*); FtsL (*green*). *C*, amino sequences of FtsB and FtsL. The residues corresponding to the predicted TM region are in *bold* with *underline*, while the CCDs and the FtsQ-interaction domain are marked. Residues among peptides with a significant uptake decrement and not covered are highlighted in *blue* and *black*, respectively. *D*, model of FtsBL subcomplex with mapped ΔHDX. Peptides showing a deuterium uptake decrement, an increment, and no significant difference are in *blue*, *red*, and *white*, respectively; while the missing fragments are in *black*. CCD, constriction control domains; HDX, hydrogen-deuterium exchange; MS, mass spectrometry; TM, transmembrane.

FtsQB and "FtsQL" complex formation

We attempted to copurify the full-length FtsQB and FtsQL subcomplexes but were unsuccessful. Instead, a set of proteins consisting of the periplasmic regions only ($FtsQ_p$, $FtsB_p$, and $FtsQ_pB_p$) were studied with the same HDX-MS method. We could not process with any FtsQL complex, presumably because this was unstable (9).

The C-terminal regions of $FtsQ_p$ (residues 194–263) and $FtsB_p$ (residues 68–84) showed significant HDX changes. Compared with the free protein, $FtsQ_p$ in the $FtsB_p$-bound state displayed a considerable deuteration decrement at the C-terminal β-domain (Fig. 3*A*), an observation consistent with those in the FtsQBL complex (Fig. 1*A*). Upon $FtsQ_p$–$FtsB_p$ interaction, the $FtsQ_p$ peptides covering residues 194 to 256 showed a maximum of 4 Da change at the 1 min time interval. These results indicated that a large portion of the $FtsQ_p$ C-terminal region is protected against deuteration and presumably more rigid in the complexed state. For $FtsB_p$, most peptides exhibited similar deuterium levels upon $FtsQ_pB_p$ complexation (Fig. 3*B*), except for those from residues 68 to 84. The uptake level of the related fragments (68–75, 76–84, and 77–84) was moderately reduced by about 1 Da in the complexed state at the 1 min time interval. In contrast, there were no detectable HDX differences in the other peptides between the free and complexed state (Fig. 3*B*). These results suggested that the $FtsQ_pB_p$ complexation affected the residues 194 to 263 in $FtsQ_p$ and 68 to 84 in $FtsB_p$.

Taking the results from the FtsQBL and $FtsQ_pB_p$ complexes together (Figs. 1 and 3), the C terminus of FtsB is likely binding to FtsQ, which in turn, also shields and/or stiffens the upper β-domain of FtsQ (residues 187–263). This observation is consistent with the recent X-ray crystallographic studies of $FtsQ_pB_p$, showing that multiple residues in FtsQ from Tyr248 to the C termini are critical for the interaction with FtsB (residues 64–87) (10, 22).

Discussion

Although the crystal structure of the FtsQ periplasmic region and some FtsB partial structures are available (10, 19, 21, 23), the structures of the full-length FtsQ, FtsB, and FtsL, either individually or in the complex state, remains unknown. The HDX-MS analyses of the full-length FtsQ, FtsB, and FtsL

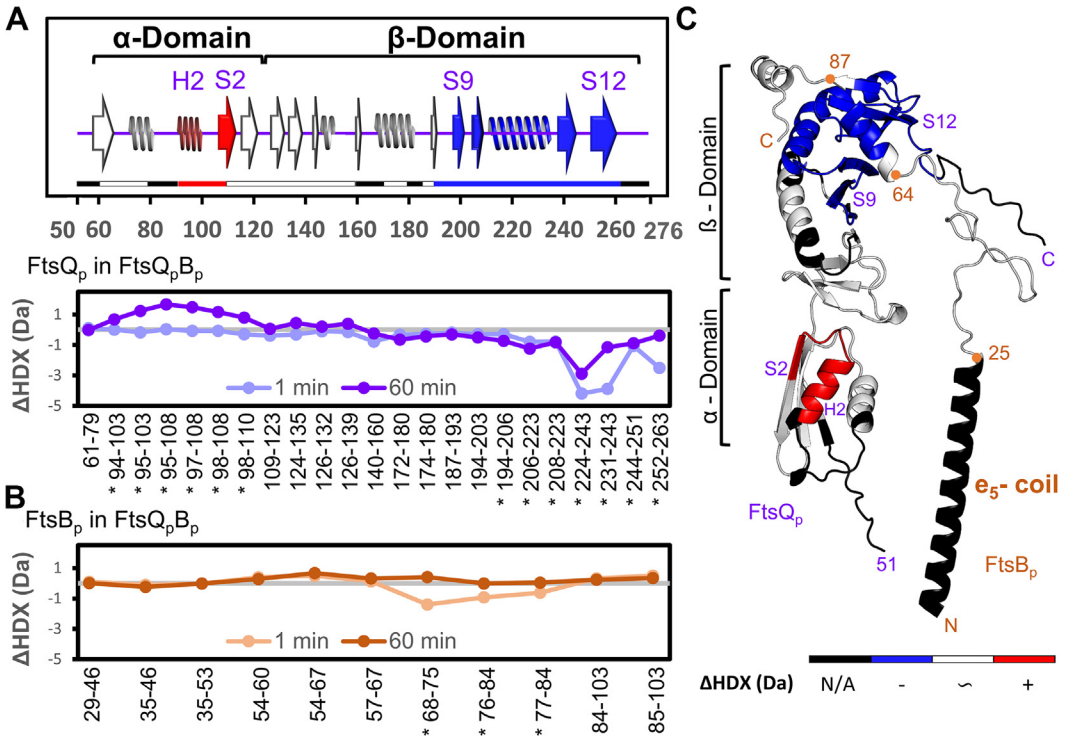

Figure 3. The dynamics of the $FtsQ_pB_p$ complex monitored by HDX-MS. The peptide deuterium uptake differences (ΔHDX, $FtsQ_pB_p$-complexed state minus the free states) of (*A*) $FtsQ_p$ with the secondary structure shown on *top* and (*B*) $FtsB_p$ at the time intervals of 1 min and 60 min. Peptides with significant ΔHDX are marked with an *asterisk*. The general coloring scheme for the ΔHDX plots of the two proteins are as follows: $FtsQ_p$ (*purple*) and $FtsB_p$ (*orange*). *C*, model of $FtsQ_pB_p$ subcomplex. Peptides showing a deuterium uptake decrement, an increment, and no difference are shown in *blue*, *red*, and *white*, respectively; while the missing fragments are in *black*. This information is also included with the same color scheme in the bar of (*A*). HDX, hydrogen-deuterium exchange; MS, mass spectrometry.

proteins in this work provided valuable information on the structural characteristics of various complexed states. Our result showed that the interactions between FtsQ–FtsB and FtsB–FtsL could be located at the C termini and the TM with the lower periplasmic regions, respectively. We did not observe any interaction between FtsL and FtsQ in the FtsQBL complex. The protection patterns in FtsL in the FtsBL (Fig. 2*B*) and the FtsQBL (Fig. 1*C*) complexes were similar. It is noteworthy that purification of the binary subcomplexes FtsQL and $FtsQ_pL_p$ both failed. Also, an assumption was made that the individual proteins were not misfolded in the condition that they could copurify in complexes.

The induced FtsB periplasmic helix in the FtsBL complex

Previous studies have predicted that FtsB is monomeric, with a flexible and unstructured periplasmic domain (12, 27). In the cocrystallization attempts of the FtsQ and FtsB periplasmic domains ($FtsQ_pB_p$), FtsB residues 22 to 63 and 88 to 103 were found to be disordered in the crystal structures (Protein Data Bank ID: 6H9N, 5Z2W) (10, 22). That is, the FtsB periplasmic region was without structure in the absence of FtsL. Our HDX-MS experiments provided additional dynamical information on the FtsB structure upon complexation. FtsB is probably mainly unstructured in the free state. The interactions with FtsL presumably facilitate the helical structure formation in FtsB, and the FtsBL complex becomes a coiled-coil structure (Fig. 4).

The FtsB periplasmic domain could be, indeed, flexible in the free state. Our data (Fig. S4*A*) showed that most FtsB fragments were fully deuterated in the first 10 s. This rapid exchange rate in the periplasmic domain (residues 22–103) implied that there is probably no rigid structure to protect the amide hydrogens. In contrast, the HDX rates were much lower in the peptides from residues −1 to 19, corresponding to the TM region (residues 4–21). Upon the interaction with FtsL, the substance HDX reduction in the FtsB lower periplasmic region (residues 22–54) presumably due to the solvent accessibility reduction and the formation of a rigid α-helix (Fig. 2). This region could be potentially induced into a helical structure (23). Recently, a computational model of the FtsBL complex has also proposed a discontinuous crossregion helix in FtsB (11). It was also suggested that the TM and the nearby periplasmic region of FtsB and FtsL are responsible for the FtsBL complex formation (27, 28, 35). It should be noted that the HDX behavior would not rule out the possibility of FtsBL or FtsQBL form in a higher oligomerization state (see Supporting information for further discussion).

The hypothesized FtsL-induced secondary structure formation in FtsB and the binding with FtsL may be critical for the establishment of the FtsQBL complex. The C terminus interaction of FtsB and FtsQ could be observed in both the FtsQBL and $FtsQ_pB_p$ complexes (Figs. 1*B* and 3*B*). Recent crystallographic studies showed that FtsB interacts with FtsQ by a helix-turn-strand motif at residues 64 to 87 (10, 22). The

Dynamic change of the FtsQ, FtsB, and FtsL complexation

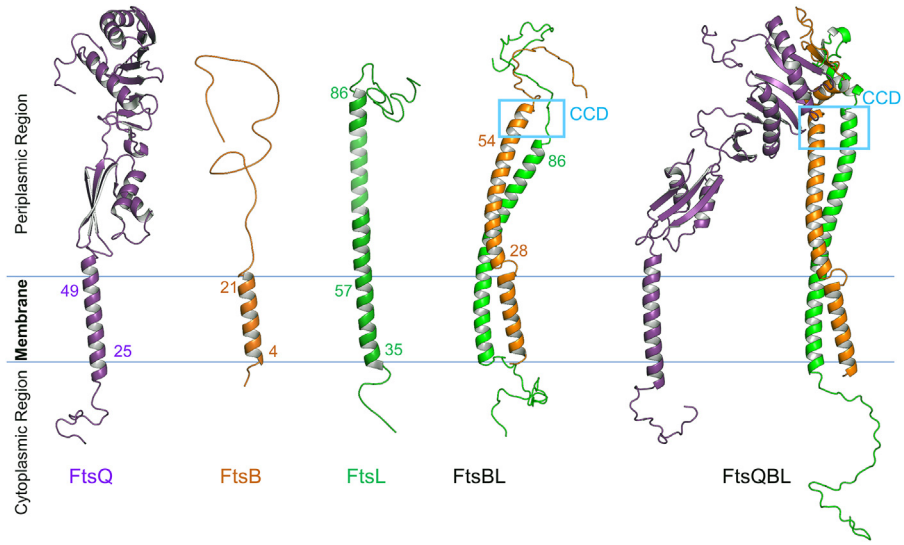

Figure 4. Models of components in the FtsQBL complex. The FtsB periplasmic domain is progressively forming substructures, depending on the state of complexation. The interactions with FtsL might induce a coiled-coil structure at the periplasmic region (FtsBL). In the FtsQBL complex, the FtsB helix-turn-strand motif binds to the FtsQ β-domain.

resulting coiled-coil structure in the FtsBL complex reduces the overall flexibility of FtsB, thus adjusting the vertical distance of the C-terminal region relative to the membrane (or detergent micelle) surface. A previous study showed that the introduction of FtsL could increase the affinity between FtsQ and FtsB (9). A recent study also showed that FtsB and FtsL form a subcomplex before interacting with FtsQ (8). CD indicated that the FtsBL complex is rich in helical content (34). Therefore, the binding with FtsL and the hypothesized rigidity enhancement of FtsB probably orientated the FtsQ-interaction motif to an optimal location that facilitates the formation of the FtsQBL complex (Fig. 4).

It is worth noting that the formation of the FtsBL subcomplex also enhances the FtsL rigidity. FtsL has been predicted as a continuous helix across the TM and the periplasmic domains (11, 23, 27), which is probably crucial for the FtsBL complexation (21, 24). The interaction with FtsB may further stabilize this long helical structure. In the free state of FtsL, 17 out of 26 peptide fragments were not fully deuterated after 10 s of labeling (Fig. S4*B*). Only five peptides from residues 49 to 62 and 78 to 86 are better protected that remained with a relatively low deuterium uptake (<75%) at the time interval of 1 min. At the same time point, the middle section (residues 63–78) is almost fully deuterated. This relatively weak protection indicated that although FtsL might contain a crossdomain helix in the free state, the FtsL periplasmic helix presumably retains certain flexibility. Upon FtsBL subcomplex formation (Fig. 2*B*), the notable HDX reduction (>1.8 Da) in FtsL could be due to a strong interaction with FtsB and/or the enhanced rigidity of FtsL resulting from FtsBL complexation.

Orientation of the CCD domain in FtsB and FtsL

Inspired by molecular modeling (refer to Supporting information), we hypothesize that the CCD domains might be brought to spatial proximity in the FtsBL complex. Our HDX result showed that the observed protection pattern started from the TM regions and ended at residues 54 in FtsB and 86 in FtsL (Fig. 2, *A* and *B*). However, the peptic peptides corresponding to the CCD domains (residues 54–60 in FtsB and 86–99 in FtsL) have indistinguishable HDX differences in both the FtsBL and FtsQBL complexes (Figs. 1, *B* and *C* and 2, *A* and *B*). Therefore, the interaction interface probably ended and did not involve the respective CCD domains (Fig. 2*C*). Moreover, the resulting FtsBL coiled-coil may restrict the distance and position of this domain relative to the membrane. This orientation of the CCD domains may be essential for regulating activity and interaction with other divisomal proteins. Although the detailed dynamics of the CCD domains remain unclear, our work provides an insight that the interaction between FtsB and FtsL might not directly involve the CCD domains but drive the CCD domains into the proper orientation for further interactions.

It was previously proposed that membrane-bound FtsBL is a Y-shaped tetramer, with two of each protein (34). The TM helices formed a four helix bundle in that model, whereas the periplasmic domains form two FtsBL coiled-coils stabilized by polar interactions between FtsB and FtsL, up to the CCD domains. Our results revealed that the protection of FtsB residues 2 to 54 and FtsL residues 33 to 86 (Fig. 2, *A* and *B*) in the FtsBL complex, which is also consistent with this model.

Alignment of FtsQ α- and β-domains in the FtsBL-bound state

Crystallographic studies showed that FtsQ interacts with FtsB at its C terminus (10, 22). Our HDX results revealed that this binding could affect a larger region (residues 187–263) of the FtsQ β-domain from S8 to S12, including the FtsB-interaction site (Figs. 1*A* and 3*A*). Interestingly, HDX reduction was also observed in the region from S3 to S5 (residues 124–139) in the full-length FtsQBL complex (Fig. 1*A*). This region is the lower β-domain in FtsQ that connects to the α-domain.

From the molecular model, we speculate that there may be a global rigidity enhancement in the FtsQ resulting from the FtsB interaction and the membrane anchorage. This increase in rigidity is reflected in the HDX change from S3 to S5, the lower β-domain, which was unlikely due to direct interaction with FtsB and FtsL. The HDX profiles of FtsB and FtsL proteins were very similar between those of the FtsBL (Fig. 2, *A* and *B*) and the FtsQBL complexes (Fig. 1, *B* and *C*), except for the C-terminal FtsQ-interaction site in FtsB. Moreover, this dynamic change in S3 to S5 cannot be found in the truncated $FtsB_p$-bound $FtsQ_p$ (Fig. 3*A*). Therefore, we speculate that the combined effects of membrane anchorage and the interaction with the detergent-embedded FtsB lead to the overall stiffening in FtsQ. As a result, the FtsQBL complexation might induce a rigid connection between the FtsQ α- and β-domains. This is supported by our molecular dynamics simulation results.

The root-mean-square fluctuation (rmsf) of the Cα atoms of the simulated model is an indication of the extent of movement, that is rigidity, of the protein backbone. We calculated the regional average rmsf of the membrane-embedded FtsQ in its free and the FtsBL-bound models and compared the values (Fig. S3). The overall Cα rmsf of the ordered region (residues 60–257) of the FtsQ periplasmic domain on its own and that in the FtsQBL complex were 2.27 ± 0.05 Å (SD = 0.80) and 1.70 ± 0.04 Å (SD = 0.62), respectively. The FtsQ periplasmic domain is thus significantly less flexible, by 0.57 ± 0.06 Å when it forms the complex. The rmsf of the FtsQ β-domain (residues 160–257) decreased to a similar extent, by 0.54 Å, in the FtsQBL state compared to that in the free state. The rmsf of the S3 to S5 hinge region (residues 124–139) was reduced by a larger degree of 0.71 Å, compared to the overall rmsf difference (Fig. S3).

A dynamic model of FtsQBL interaction

We successfully identified the residues, at the peptide fragment level, in the full-length FtsQ, FtsB, and FtsL proteins that might be involved in the complex formation. Analysis of the HDX profiles has shown that the flexible FtsB periplasmic domain undergoes a drastic structural change after interacting with the relatively rigid FtsL. Combined with the knowledge acquired from previous studies, a helical structure is probably induced in the FtsB periplasmic region (Fig. 4). FtsB and FtsL interact extensively through a region involving a range of residues from the TM and periplasmic domains in both proteins. An FtsBL coiled-coil model can be built with the two CCDs in the two proteins brought into close proximity. The vertical distance between the two CCD domains and the membrane surface may be defined and fixed by the formation of the coiled-coil. This structural integrity enhancement may also position the FtsQ-interaction region in FtsB into an optimal location for binding. The FtsQB interactions at the C termini stiffen the upper β-domain in FtsQ (from S8 to S12). With the TM domain, additional rigidity augmentation in the region from S3 to S5 in FtsQ is achieved. The interaction with FtsBL probably further stiffens FtsQ and optimally aligns its α- and β-domains. To sum up, the flexible and partially unstructured individual FtsB form a rigid and structurally well-defined FtsBL complex with the orientated CCD domains and the α- and β-domains of FtsQ optimally primed for the divisome regulation in the three-member complex.

Experimental procedures

Materials

Chemicals for protein purification were of biological grade or similar purchased from Sigma–Aldrich and used without further purification. Primers were ordered from HK Primer (Life Technologies, Thermo Fisher Scientific). The synthetic genes encoding the sequences of His_6-TEV-e_5-$FtsB_p$ were obtained from BGI (Hong Kong Co Limited). The deuterium oxide was bought from Cambridge Isotope Laboratories.

Protein expression, purification, and characterization

His-tagged periplasmic and full-length Fts-proteins were (co) expressed and (co)purified according to the methods reported by the previous literature from Marjolein Glas (9) and Adrien Boes (12). In brief, free and the corresponding Fts-protein complexes were (co)expressed in *E. coli* BL21 (DE3) or C43 (DE3) harboring the transformed plasmid(s). The copurifications were achieved using the His-tagged FtsB or $FtsB_p$ as bait.

Bacteria were first grown in LB medium with ampicillin at 37 °C for 12 h. The culture was then diluted into 2xTY medium (with ampicillin) in a 1:50 volume ratio and then incubated at 37 °C. Once the A_{600} reached 0.8, the expression was induced by a final concentration of 1 mM IPTG at 16 °C for 14 h. Cells were collected by centrifugation followed by resuspension with protease inhibitor cocktail (cOmplete, Sigma–Aldrich) in lysis buffer and lysed by the cell disruptor (TS2, Constant system LTD). Different lysis buffers were used for the periplasmic protein $FtsQ_p/B_p/L_p$ (50 mM sodium phosphate pH 8.0, 300 mM NaCl, 10 mM imidazole, 10 mM DTT, and 1 mM PMSF) and the full-length FtsQ/B/L proteins (50 mM Tris–HCL pH 7.5, 50 mM NaCl). The debris was then removed by centrifugation (2 h, 10,864*g*, 4 °C). The $FtsQ_p/B_p/L_p$ proteins in the acquired supernatant were directly purified in the next step. For the membrane-bound FtsQ/B/L proteins, supernatants were recovered and subjected to an additional ultracentrifugation step (1 h, 276,900*g*, 4 °C). The membrane proteins were then collected in pellets and extracted by agitation in solubilizing buffer (50 mM HEPES, pH 7.5, 500 mM NaCl, 10% (v/v) glycerol, 30 mM *n*-dodecyl-β-D-maltopyranoside [DDM]) for further purification. Target proteins from both constructs were purified by Ni-NTA agarose resins (Qiagen). Individual proteins and protein complexes were (co)purified by imidazole in a stepwise concentration: of 20 mM, 140 mM, 200 mM, and 400 mM. Protein purities and their molecular weights were analyzed by standard SDS-PAGE and LC-MS. Amicon (Merck) was used to concentrate and buffer exchange the purified periplasmic proteins (50 mM ammonium acetate) and the full-length protein (50 mM HEPES, pH 7.5, 300 mM NaCl, 1 mM DDM). All buffer used for the full-length proteins was supplemented with 1 mM DDM to warrant the micelle formation with a critical minimum concentration of 0.17 mM.

Dynamic change of the FtsQ, FtsB, and FtsL complexation

HDX-MS

The HDX-MS was conducted with a Waters Synapt G2-Si Mass Spectrometer equipped with an automated HDX manager (LEAP technologies). Deuterium labeling was performed by adding 5 μl of protein sample (40 μM) to 95 μl of deuterium buffer (pD 7.0, 50 mM potassium phosphate in 99.9% D_2O). Proteins were deuterated at room temperature (RT) in selected on-exchange periods. After each interval, the exchange reaction was quenched by transferring the deuterated sample to a quenching buffer (pH 2.5, 50 mM potassium phosphate) in a 1:1 volume ratio that was kept at 0 °C. A 50 μl portion of the quenched sample was injected immediately into ultra-performance liquid chromatography (UPLC)–MS. Proteins were first digested online, followed by 3 min of concentrating and desalting at the guard column (ACQUITY UPLC BEH C18 VanGuard Pre-column, 130 Å, 1.7 μm, 2.1 mm × 5 mm). The digested peptides were then separated through the C18 reverse-phase analytical column (ACQUITY UPLC BEH C18 Column, 130 Å, 1.7 μm, 1 mm × 100 mm) using 10% to 95% water:acetonitrile (with 0.1% (v/v) formic acid) solvent gradient. The peptides were separated and eluted with a solvent gradient of 0 to 0.5 min: 92% A/8% B, 0.5 to 10 min: 92% A/8% B to 40% A/60% B, 10 min to 10.5 min: 40% A/60% B to 5% A/95% B, 10.5 min to 13.5 min: 5% A/95% B, where solvent A was H2O with 0.1% formic acid and solvent B was acetonitrile with 0.1% formic acid. The solvent flow rate was 60 μl/min. To minimize back exchange, except for the pepsin column (Waters Enzymate BEH Pepsin Column, 300 Å, 5 μm, 2.1 mm × 30 mm) was kept at RT, all parts of the Acquity UPLC M-Class dual-pump LC system were placed in a 0 °C chamber. The eluted peptides were analyzed with the mass spectrometer (MS^E data acquisition mode) using leucine enkephalin for internal mass calibration. The mass spectrometer conditions were: 3 kV capillary voltage, 150 °C source temperature, 350 °C desolvation temperature, 600 l/h of desolvation gas flow, and 6.5 bar nebulizer gas flow. The mass spectrometer was operated in MSe mode with a 0.3 s scan time. The trap collision energy was ramped with a 6 V lower energy acquisition and 15 to 35 V for high energy acquisition. Three technical replicates were performed for each HDX time point. Six column volume of pepsin wash solution (1.5 M guanidine hydrochloride/acetonitrile/formic acid in 4.0/95.2/0.8% (v/v)) was injected to clean the pepsin column, and the same solvent gradient was used subsequently to remove the residual peptides in the C18 column after each sample injection. Various parameters of the HDX-MS experiments are summarized in Table S2.

HDX-MS data analysis

Peptide peak assignment was performed by the ProteinLynx Global Server (PLGS, version 3.0.2, Waters) with the primary sequence of the target proteins. Only the peptide that matched the following criteria were processed: PLGS score >6, precursor ion (MH+) mass error <10 ppm, and the number of product ions per amino acid >0.33. The HDX-MS data of the free and complexed Fts-proteins were processed by the DynamX (Version 3.0.0, Waters) software, and the results were manually inspected. An *E coli* proteome (GCF_012978145.1) database was used to validate the peptide assignment. The reference mass of each peptide was generated by the same HDX-MS procedure while replacing all the D_2O with deionized water. There is no bimodal distribution in the analyzed peptides. The average deviation of the deuterium uptake was below 0.1 Da. Back exchange level was estimated to be an average rate of 50% by analyzing fully deuterated peptides and was not corrected when carrying out comparisons of deuterium uptake.

Model construction

The detail of molecular modeling is included in the supporting information (Table S1, Figs. S1 and S2).

Data availability

All data relevant to this work are contained within this article and the associated supporting information. MS data are available in ProteomeXchange *via* the PRIDE (39) partner repository with identifier PXD031342.

Supporting information—This article contains supporting information (9–11, 19, 22, 23, 33, 34, 40–43).

Acknowledgments—We acknowledge the support from the Research Grants Council (Grant No. 15305217) and the Innovation and Technology Commission.

Author contributions—W.-P. K., F. G., P.-K. S., and K.-Y. W. conceptualization; W.-P. K., F. G., P.-K. S., and K.-Y. W. methodology; P.-K. S. validation; W.-P. K., F. G., and P.-K. S. formal analysis; W.-P. K., F. G., and P.-K. S. investigation; Y.-C. L. and K.-Y. W. resources; W.-P. K. and F. G. data curation; W.-P. K., and F. G. writing-original draft; K.-Y. W. writing-review and editing; W.-P. K. visualization; Y.-C. L. and K.-Y. W. supervision; K.-Y. W. project administration; Y.-C. L. and K.-Y. W. funding acquisition.

Funding and additional information—K.-Y. W. acknowledges the support from the Patrick S.C. Poon Endowed Professorship. Support from the University Research Facility in Chemical and Environmental Analysis and the University Research Facility in Life Sciences of The Hong Kong Polytechnic University are also gratefully acknowledged.

Conflict of interest—The authors declare that they have no conflicts of interest with the contents of this article.

Abbreviations—The abbreviations used are: CCD, constriction control domains; HDX, hydrogen-deuterium exchange; MS, mass spectrometry; rmsf, root-mean-square fluctuation; sPG, septal-peptidoglycan; TM, transmembrane; UPLC, ultra-performance liquid chromatography.

References

1. Park, K. T., Du, S., and Lutkenhaus, J. (2020) Essential role for FtsL in activation of septal peptidoglycan synthesis. *mBio* **11**, e03012-20
2. Du, S., and Lutkenhaus, J. (2017) Assembly and activation of the Escherichia coli divisome. *Mol. Microbiol.* **105**, 177–187

3. Goehring, N. W., Gonzalez, M. D., and Beckwith, J. (2006) Premature targeting of cell division proteins to midcell reveals hierarchies of protein interactions involved in divisome assembly. *Mol. Microbiol.* **61**, 33–45
4. Natale, P., Pazos, M., and Vicente, M. (2013) The Escherichia coli divisome: born to divide. *Environ. Microbiol.* **15**, 3169–3182
5. Trip, E. N., and Scheffers, D. J. (2015) A 1 MDa protein complex containing critical components of the Escherichia coli divisome. *Sci. Rep.* **5**, 18190
6. Liu, B., Persons, L., Lee, L., and de Boer, P. A. J. (2015) Roles for both FtsA and the FtsBLQ subcomplex in FtsN-stimulated cell constriction in Escherichia coli. *Mol. Microbiol.* **95**, 945–970
7. den Blaauwen, T., Hamoen, L. W., and Levin, P. A. (2017) The divisome at 25: the road ahead. *Curr. Opin. Microbiol.* **36**, 85–94
8. Buddelmeijer, N., and Beckwith, J. (2004) A complex of the Escherichia coli cell division proteins FtsL, FtsB and FtsQ forms independently of its localization to the septal region. *Mol. Microbiol.* **52**, 1315–1327
9. Glas, M., van den Berg van Saparoea, H. B., McLaughlin, S. H., Roseboom, W., Liu, F., Koningstein, G. M., *et al.* (2015) The soluble periplasmic domains of Escherichia coli cell division proteins FtsQ/FtsB/FtsL form a trimeric complex with submicromolar affinity. *J. Biol. Chem.* **290**, 21498–21509
10. Choi, Y., Kim, J., Yoon, H. J., Jin, K. S., Ryu, S., and Lee, H. H. (2018) Structural insights into the FtsQ/FtsB/FtsL complex, a key component of the divisome. *Sci. Rep.* **8**, 18061
11. Condon, S. G. F., Mahbuba, D. A., Armstrong, C. R., Diaz-Vazquez, G., Craven, S. J., LaPointe, L. M., *et al.* (2018) The FtsLB subcomplex of the bacterial divisome is a tetramer with an uninterrupted FtsL helix linking the transmembrane and periplasmic regions. *J. Biol. Chem.* **293**, 1623–1641
12. Boes, A., Olatunji, S., Breukink, E., and Terrak, M. (2019) Regulation of the peptidoglycan polymerase activity of PBP1b by antagonist actions of the core divisome proteins FtsBLQ and FtsN. *mBio* **10**, e01912-18
13. Tsang, M. J., and Bernhardt, T. G. (2015) A role for the FtsQLB complex in cytokinetic ring activation revealed by an ftsL allele that accelerates division. *Mol. Microbiol.* **95**, 925–944
14. Muller, P., Ewers, C., Bertsche, U., Anstett, M., Kallis, T., Breukink, E., *et al.* (2007) The essential cell division protein FtsN interacts with the murein (peptidoglycan) synthase PBP1B in Escherichia coli. *J. Biol. Chem.* **282**, 36394–36402
15. Gerding, M. A., Liu, B., Bendezu, F. O., Hale, C. A., Bernhardt, T. G., and de Boer, P. A. (2009) Self-enhanced accumulation of FtsN at division sites and roles for other proteins with a SPOR domain (DamX, DedD, and RlpA) in Escherichia coli cell constriction. *J. Bacteriol.* **191**, 7383–7401
16. Scheffers, D. J., Robichon, C., Haan, G. J., den Blaauwen, T., Koningstein, G., van Bloois, E., *et al.* (2007) Contribution of the FtsQ transmembrane segment to localization to the cell division site. *J. Bacteriol.* **189**, 7273–7280
17. Guzman, L. M., Weiss, D. S., and Beckwith, J. (1997) Domain-swapping analysis of FtsI, FtsL, and FtsQ, bitopic membrane proteins essential for cell division in Escherichia coli. *J. Bacteriol.* **179**, 5094–5103
18. Carson, M. J., Barondess, J., and Beckwith, J. (1991) The FtsQ protein of Escherichia coli: membrane topology, abundance, and cell division phenotypes due to overproduction and insertion mutations. *J. Bacteriol.* **173**, 2187–2195
19. Van Den Ent, F., Vinkenvleugel, T. M., Ind, A., West, P., Veprintsev, D., Nanninga, N., *et al.* (2008) Structural and mutational analysis of the cell division protein FtsQ. *Mol. Microbiol.* **68**, 110–123
20. Sánchez-Pulido, L., Devos, D., Genevrois, S., Vicente, M., and Valencia, A. (2003) POTRA: a conserved domain in the FtsQ family and a class of β-barrel outer membrane proteins. *Trends Biochem. Sci.* **28**, 523–526
21. D'Ulisse, V., Fagioli, M., Ghelardini, P., and Paolozzi, L. (2007) Three functional subdomains of the Escherichia coli FtsQ protein are involved in its interaction with the other division proteins. *Microbiology (Reading)* **153**, 124–138
22. Kureisaite-Ciziene, D., Varadajan, A., McLaughlin, S. H., Glas, M., Monton Silva, A., Luirink, R., *et al.* (2018) Structural analysis of the interaction between the bacterial cell division proteins FtsQ and FtsB. *mBio* **9**, e01346-18
23. LaPointe, L. M., Taylor, K. C., Subramaniam, S., Khadria, A., Rayment, I., and Senes, A. (2013) Structural organization of FtsB, a transmembrane protein of the bacterial divisome. *Biochemistry* **52**, 2574–2585
24. Den Blaauwen, T., and Luirink, J. (2019) Checks and balances in bacterial cell division. *mBio* **10**, e00149-19
25. Villanelo, F., Ordenes, A., Brunet, J., Lagos, R., and Monasterio, O. (2011) A model for the Escherichia coli FtsB/FtsL/FtsQ cell division complex. *BMC Struct. Biol.* **11**, 28
26. Buddelmeijer, N., and Beckwith, J. (2002) Assembly of cell division proteins at the E. coli cell center. *Curr. Opin. Microbiol.* **5**, 553–557
27. Khadria, A. S., and Senes, A. (2013) The transmembrane domains of the bacterial cell division proteins FtsB and FtsL form a stable high-order oligomer. *Biochemistry* **52**, 7542–7550
28. Robichon, C., Karimova, G., Beckwith, J., and Ladant, D. (2011) Role of leucine zipper motifs in association of the Escherichia coli cell division proteins FtsL and FtsB. *J. Bacteriol.* **193**, 4988–4992
29. Masson, G. R., Burke, J. E., Ahn, N. G., Anand, G. S., Borchers, C., Brier, S., *et al.* (2019) Recommendations for performing, interpreting and reporting hydrogen deuterium exchange mass spectrometry (HDX-MS) experiments. *Nat. Methods* **16**, 595–602
30. Giladi, M., and Khananshvili, D. (2020) Hydrogen-deuterium exchange mass-spectrometry of secondary active transporters: from structural dynamics to molecular mechanisms. *Front. Pharmacol.* **11**, 70
31. Li, X., Eyles, S. J., and Thompson, L. K. (2019) Hydrogen exchange of chemoreceptors in functional complexes suggests protein stabilization mediates long-range allosteric coupling. *J. Biol. Chem.* **294**, 16062–16079
32. Benhaim, M., Lee, K. K., and Guttman, M. (2019) Tracking higher order protein structure by hydrogen-deuterium exchange mass spectrometry. *Protein Pept. Lett.* **26**, 16–26
33. Huang, L., So, P. K., Chen, Y. W., Leung, Y. C., and Yao, Z. P. (2020) Conformational dynamics of the helix 10 region as an allosteric site in class A beta-lactamase inhibitory binding. *J. Am. Chem. Soc.* **142**, 13756–13767
34. Craven, S. J., Condon, S. G. F., Diaz Vazquez, G., Cui, Q., and Senes, A. (2022) The coiled-coil domain of Escherichia coli FtsLB is a structurally detuned element critical for modulating its activation in bacterial cell division. *J. Biol. Chem.* **298**, 101460
35. Gonzalez, M. D., Akbay, E. A., Boyd, D., and Beckwith, J. (2010) Multiple interaction domains in FtsL, a protein component of the widely conserved bacterial FtsLBQ cell division complex. *J. Bacteriol.* **192**, 2757–2768
36. Narang, D., James, D. A., Balmer, M. T., and Wilson, D. J. (2021) Protein footprinting, conformational dynamics, and core interface-adjacent neutralization "hotspots" in the SARS-CoV-2 spike protein receptor binding domain/human ACE2 interaction. *J. Am. Soc. Mass Spectrom.* **32**, 1593–1600
37. Guzman, L. M., Barondess, J. J., and Beckwith, J. (1992) FtsL, an essential cytoplasmic membrane protein involved in cell division in Escherichia coli. *J. Bacteriol.* **174**, 7716–7728
38. Gonzalez, M. D., and Beckwith, J. (2009) Divisome under construction: distinct domains of the small membrane protein FtsB are necessary for interaction with multiple cell division proteins. *J. Bacteriol.* **191**, 2815–2825
39. Perez-Riverol, Y., Bai, J., Bandla, C., García-Seisdedos, D., Hewapathirana, S., Kamatchinathan, S., *et al.* (2022) The PRIDE database resources in 2022: a hub for mass spectrometry-based proteomics evidences. *Nucleic Acids Res.* **50**, D543–D552
40. Mirdita, M., Schütze, K., Moriwaki, Y., Heo, L., Ovchinnikov, S., and Steinegger, M. (2022) ColabFold: making protein folding accessible to all. *Nat. Methods* **19**, 679–682
41. Jumper, J., Evans, R., Pritzel, A., Green, T., Figurnov, M., Ronneberger, O., *et al.* (2021) Highly accurate protein structure prediction with AlphaFold. *Nature* **596**, 583–589
42. Abraham, M. J., Murtola, T., Schulz, R., Páll, S., Smith, J. C., Hess, B., *et al.* (2015) GROMACS: high performance molecular simulations through multi-level parallelism from laptops to supercomputers. *SoftwareX* **1**, 19–25
43. Lee, J., Cheng, X., Jason, M., Yeom, M. S., Eastman, P. K., Lemkul, J. A., *et al.* (2016) CHARMM-GUI input generator for NAMD, GROMACS, AMBER, OpenMM, and CHARMM/OpenMM simulations using the CHARMM36 additive force field. *J. Chem. Theory Comput.* **12**, 405–413